## PAPER

# Plasticized and salt-doped single-ion conducting polymer electrolytes for lithium batteries

Pedram Ghorbanzade, [ID] [ab] Laura C. Loaiza [ID] [c] and Patrik Johansson [ID] *[cd]

Single-ion conducting polymer electrolytes created by plasticizing LiPSTFSI with PPO and LiTFSI are shown to both improve the ionic conductivity and alter the ion conduction mechanism. This correlates with both local and macroscopic properties, opening for rational design of solid-state, but yet pliable electrolytes.

One of the utmost important properties of any lithium battery electrolyte is the Li transport number ($t_{Li^+}$); the fraction of the total current carried by the $Li^+$ cations. In most solid polymer electrolytes (SPEs), $t_{Li^+}$ is <0.5 due to the cations' interactions with the polymer chains, while the "free" migration of anions in the opposite direction creates concentration gradients. Approaching $t_{Li^+} = 1$ would not only reduce the these gradients, it would also improve the electrode/electrolyte interface in general, suppress the Li-dendrite growth, and allow cells to operate at higher charge–discharge rates.[1–3]

One strategy to increase $t_{Li^+}$ is by grafting the anion to the polymer chain, allowing the $Li^+$ cation to (relatively) move more freely. This type of SPE is known as single-ion conducting polymer electrolytes (SICs). One common SIC is LiPSTFSI (poly(trifluoromethane)sulfonimide lithium styrene)[4] in which an $–SO_2N^{(-)}SO_2CF_3$ anionic unit ("TFSI") is attached to a polystyrene (PS) backbone. LiPSTFSI is completely amorphous, but as the $Li^+$ cations are rather immobile, the ionic conductivity is quite low (<$10^{-8}$ S cm$^{-1}$).[4] Several attempts have been made to facilitate the ion transport in LiPSTFSI based systems, foremost by plasticizing by copolymerizing or blending with flexible polymer chains, such as PEO, poly(ethylene oxide), or its analogues.[5–9] For instance, Martinez *et al.*[7] reported an improved conductivity reaching $4.5 \times 10^{-6}$ S cm$^{-1}$ at 70 °C for a PEO–LiPSTFSI blend, while an ionic conductivity >$10^{-5}$ S cm$^{-1}$ at 60 °C was obtained by Bouchet *et al.*[9] for a triblock co-polymer of LiPSTFSI–PEO–LiPSTFSI.

Here we first of all use the fact that PPO (poly(propylene oxide)) and PEO have similar chemical structure. They both possess an ether oxygen atom in their repeating unit as a coordination site for $Li^+$, but while PEO is semi-crystalline, the additional methyl group in PPO makes it fully amorphous. Since the ion conduction in SPEs in general takes place in the amorphous phase,[1] PPO is, as a first approximation, a promising plasticizer for LiPSTFSI. Another promising route to plasticize LiPSTFSI is by adding a Li-salt, foremost to increase the number of charge carriers to remedy the dilution otherwise unavoidable. Furthermore, adding a large amount of salt will transpose the system to a polymer-in-salt[10] one and the ion transport to rely more on aggregates and clusters.[11] By choosing LiTFSI as the salt synergies are achieved by the similarity of the TFSI anion with the anionic unit of LiPSTFSI and its bulky and flexible nature, plasticizing the system, which effectively improves the ion transport.[12] However, too high salt contents may restrict the mobility of the individual charge carriers[13,14] and reduce the mechanical properties.

Herein, we report both on binary electrolytes (B##0) of LiPSTFSI (specific polymers) doped with PPO ($M_w = 4000$ g mol$^{-1}$, Alfa Aesar) and ternary electrolytes (T###) where also LiTFSI (Solvionic, dried at 110 °C overnight) is included in the composition (Table 1). All electrolytes were prepared using a 2 : 1 (v/v) mixture of acetonitrile and ethanol as secondary solvents, and then dried in a vacuum oven at 110 °C overnight. All were studied by differential scanning calorimetry (DSC) and Raman and electrochemical impedance spectroscopies.

The DSC traces were recorded on a TA instruments DSC250 under He atmosphere, between −170 °C to 170 °C, with 10 °C min$^{-1}$ rate and 20 min isothermal at the end temperatures to control the thermal history of the sample. The FT-Raman spectra were recorded on Bruker MultiRam at room temperature using a Nd-YAG 1064 nm laser at an operating power of 400 mW, with a 2 cm$^{-1}$ resolution and 4000 scans between 200 and 3200 cm$^{-1}$. The spectra were deconvoluted using PeakFit™.

Electrochemical impedance spectroscopy (EIS) was carried out using a Biologic Intermediate Temperature System (ITS) impedance analyser. The samples were placed inside a controlled environment sample holder (CESH) with gold electrodes and spectra recorded from 1 MHz to 10 mHz, with an

*[a]Centre for Cooperative Research on Alternative Energies (CIC EnergiGUNE), Basque Research and Technology Alliance (BRTA), Alava Technology Park, Albert Einstein 48, 01510 Vitoria-Gasteiz, Spain*

*[b]University of Basque Country (UPV/EHU), Barrio Sarriena, s/n, 48940 Leioa, Spain*

*[c]Department of Physics, Chalmers University of Technology, Göteborg SE-41296, Sweden. E-mail: patrik.johansson@chalmers.se*

*[d]ALISTORE-European Research InstituteFR CNRS 3104, Hub de l'Energie, 15 Rue Baudelocque, Amiens 80039, France*

Table 1 Electrolyte acronyms and compositions[a]

| Acronym | Composition[a] (%) | | | [Li$^+$] (wt%) |
|---|---|---|---|---|
| | LiPSTFSI | PPO | LiTFSI | |
| B820 | 80 | 20 | 0 | 0.011 |
| B640 | 60 | 40 | 0 | 0.008 |
| B460 | 40 | 60 | 0 | 0.005 |
| T825 | 80 | 20 | 50 | 0.690 |
| T827 | 80 | 20 | 67 | 1.483 |
| T642 | 60 | 40 | 20 | 0.321 |
| T645 | 60 | 40 | 50 | 0.906 |
| T647 | 60 | 40 | 67 | 1.315 |
| T465 | 40 | 60 | 50 | 0.690 |
| T466 | 40 | 60 | 60 | 0.905 |
| T467 | 40 | 60 | 67 | 1.071 |

[a] The compositions for T### are always calculated with respect to LiPSTFSI in a binary mixture and thus the totals are always >100%.



Fig. 1 (a) DSC traces for a few selected electrolytes, and illustrative interactions for (b) low and (c) high PPO content electrolytes.

excitation voltage of 50 mV, from 30 °C to 90 °C with 10 °C intervals. The spectra were analysed using ZView® software to fit to equivalent circuits; a R1//CPE1 in series with a CPE2 were used to model the semicircle and the straight line, respectively. The ionic conductivities were calculated from the obtained resistances using eqn (1), where $D$ is the sample thickness and $A$ the surface area:

$$\sigma = \frac{D}{R\,A} \qquad (1)$$

Eqn (2) and (3) (VTF and Arrhenius, respectively) were used to fit the ionic conductivity temperature dependent data:

$$\sigma = AT^{1/2} \exp \frac{B}{T - T_0} \qquad (2)$$

$$\sigma = \sigma_0 \exp \frac{E_a}{R\,T} \qquad (3)$$

where for eqn (2) $T_0$, the equilibrium glass transition temperature, is a reference, usually ca. 50 K below $T_g$, $B$ is the pseudo activation energy, here for the segmental motions of the polymer backbone and $A$ is a constant. In eqn (3) $E_a$ is the activation energy for migration of single or groups of ions, $\sigma_0$ is the pre-exponential factor and $R$ is the gas constant.

Since both LiPSTFSI and PPO are fully amorphous, no melting transition was expected, nor is visible in the DSC traces (Fig. 1a). The $T_g$ for low PPO content electrolytes are >150 °C and this suggests formation of dynamically crosslinked networks, which is confirmed by the high rigidity (by the eye) as "all" PPO ether oxygen atoms are coordinated by the Li$^+$ cations (Fig. 1b). For higher PPO contents the crosslinking and the resulting restricted polymer chain flexibility is less severe since many segments are free to move (Fig. 1c) – in agreement with the DSC results (Fig. 1a).

Yet, even with 60% of PPO (B460), the improvement in ionic conductivity was insignificant, still <10$^{-9}$ S cm$^{-1}$. One likely reason is the reduced Li$^+$ concentration (Table 1) as LiPSTFSI is the only source of Li and this is further diluted by the PPO

doping. In comparison and to get a perspective, a standard 1 M liquid lithium-ion battery electrolyte equals ca. 0.5 wt% Li$^+$.

Therefore, we henceforth turn to the ternary electrolytes, and indeed, the highly LiTFSI doped electrolytes were soft and gel-like in appearance and the $T_g$ decreased (Fig. 1a), confirming the plasticizing effect of LiTFSI. As a side-note they were somewhat more difficult to handle.

A complication of the ternary electrolytes is phase separation; as LiTFSI is added, the electrolytes are even visually phase separated. While the Li$^+$ cations are preferentially coordinated by the free ether oxygen atoms of PPO, once all these sites are occupied, solvent-separated and contact ion pairs and higher aggregates will start to form and eventually phase separation occurs. Such a micro- or nano-phase separation is a common phenomenon of PPO based electrolytes, comes along with double $T_g$ in the DSC traces and affects the ionic conductivity in a negative way.[15,16]

The Raman spectra of the electrolyte provide information on the ion-polymer and ion–ion interactions, and here special attention was given to the TFSI "all-breathing" mode (ca. 740 cm$^{-1}$), sensitive to both conformational[17] and coordination[18] changes.

In brief, addition of PPO increases the "free" TFSI as the Li$^+$ cations preferably interact with the ether oxygen atoms of PPO (Fig. 2a). The addition of LiTFSI more or less has the same result and for the same reasons, with LiTFSI dissociating (Fig. 2b). However, for higher LiTFSI contents, PPO can no longer coordinate more Li$^+$ and thus not dissociate LiTFSI, and as a result, aggregates form (Fig. 2c). Somewhat speculative, this decrease in "free" TFSI should indicate anions less mobile and thus improved $t_{Li^+}$. As the TFSI band includes both the TFSI coming from LiTFSI and "TFSI" from LiPSTFSI the analysis cannot be made unambiguously.
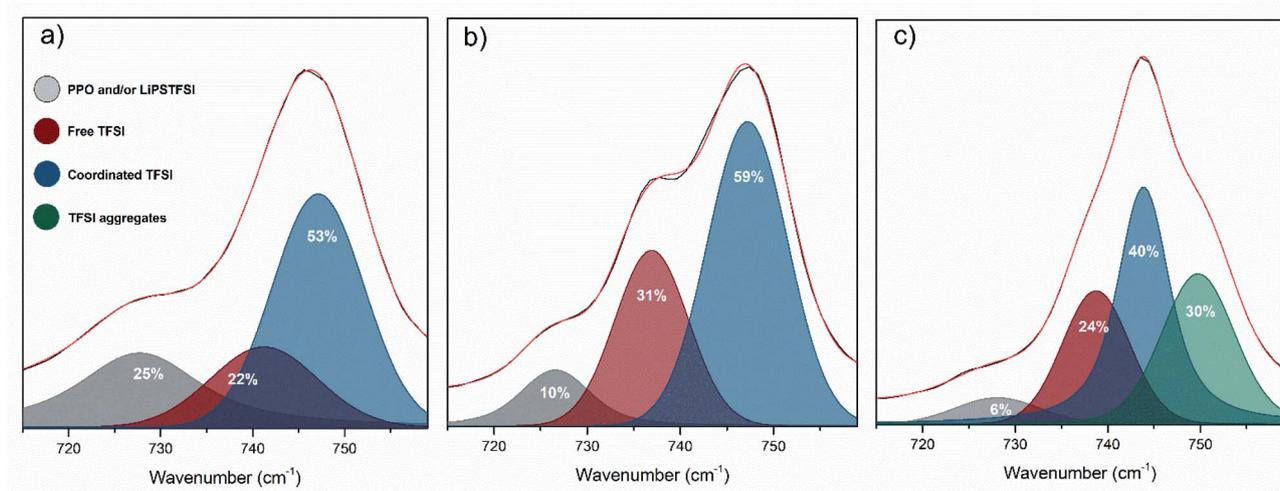
**Fig. 2** Deconvolution of the TFSI "all-breathing" band in the Raman spectra of: (a) B640, (b) T642, and (c) T645.
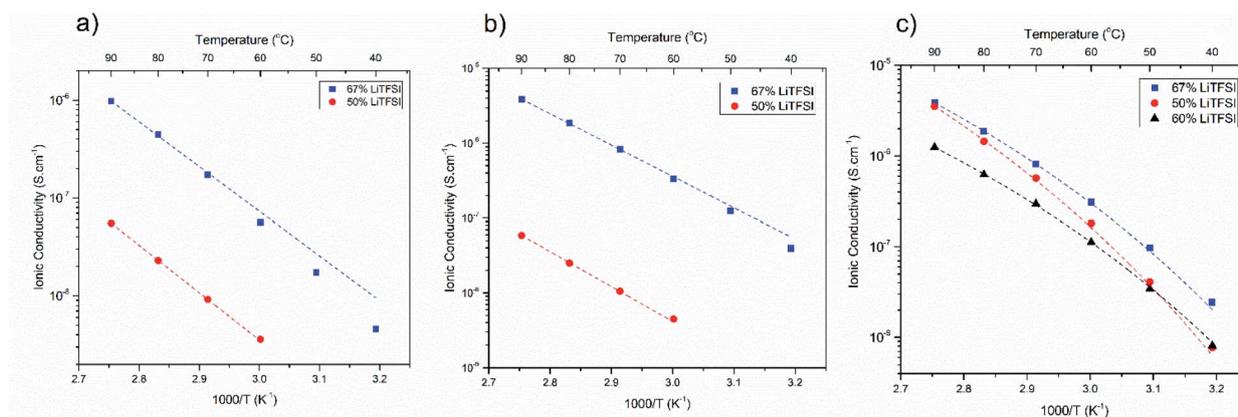


**Fig. 3** Arrhenius plots of ionic conductivity for: (a) T825 and T827, (b) T645 and T647, and (c) T465, T466 and T467.

For the ternary electrolytes the fitting of the temperature dependence of the ionic conductivities show that T827 and T647, *i.e.* with 20 and 40% PPO, respectively, predominantly have an Arrhenius conduction mechanism, while for those electrolytes with higher PPO contents, T467 and T466, the data correlate better with a VTF conduction mechanism (Fig. 3). None of the changes are sharp and most likely both conduction mechanisms are present for a wide range of electrolytes, but to different extent, due to their very nature.

From a practical perspective, higher LiTFSI contents improved the ionic conductivity, excepted T466 (Fig. 3, Table 2). The latter might be due to a phase separation and formation of LiPSTFSI-poor and -rich regions. Overall, however, ionic conductivity increases, by almost 2 orders of magnitude, were made possible by the combined plasticization of PPO and TFSI and charge carrier addition *via* the LiTFSI salt.

Unfortunately, the rather bad mechanical properties and the non-free-standing nature of our electrolytes make it difficult to perform tests such as Li plating/stripping to corroborate the

improved performance of the polymer and salt-doped electrolytes, as well as *e.g.* determine $Li^+$ transport numbers electrochemically. This highlights the significance of the mechanical properties, which needs to be further addressed by optimizing the molecular weight and/or switching to PEO–PPO copolymers to achieve self-standing yet soft membranes, or by modifying the chemical structure of the plasticizer.

**Table 2** Some properties of the ternary electrolytes

| Acronym | $T_g$ (°C) | $\sigma_{90\,°C}$ (S cm$^{-1}$) | Conduction mechanism |
| --- | --- | --- | --- |
| T825 | −4 | $5.5 \times 10^{-8}$ | Arrhenius |
| T827 | −11 | $9.7 \times 10^{-7}$ | Arrhenius |
| T645 | −1 | $5.9 \times 10^{-8}$ | Arrhenius |
| T647 | −8 | $3.9 \times 10^{-6}$ | Arrhenius |
| T465 | 26 | $3.5 \times 10^{-6}$ | VTF |
| T466 | 4 | $1.3 \times 10^{-6}$ | VTF |
| T467 | 4 | $3.9 \times 10^{-6}$ | VTF |

# Concluding remarks

Plasticization combined with (Li)salt-doping as an approach to increase the ionic conductivity of SICs was investigated. Improving the polymer flexibility by addition of amorphous PPO does clearly not suffice to improve the ionic conductivity significantly, likely due to the reduced charge carrier concentration. However, this can successfully be mitigated by doping also with LiTFSI, rendering soft and pliable ternary electrolytes, with effectively increased ionic conductivities. Our present approach and choice of materials appears to be a good strategy to simultaneously increase the ionic conductivity and the flexibility of the polymer matrix, while avoiding any formation of crystalline phases, as *e.g.* opposed to doping with PEO. While our obtained ionic conductivities are lower even when compared to standard SPEs, they are in the range of most similar SICs. However, the complex trade-offs needed to be made between polymer flexibility and mechanical properties, and possibly also $t_{Li^+}$, should not be disregarded.

Some future perspectives are to further investigate the local dynamics and diffusion by NMR spectroscopy and to copolymerize LiPSTFSI with PPO, in order to prevent phase separation even at high salt contents. Another route could be to study and understand the effect of different PPO molecular weights on both the ion conduction mechanism and the practicalities of SIC processing.

# Conflicts of interest

There are no conflicts to declare.

# Acknowledgements

# Notes and references

1 G. G. Eshetu, M. Armand and S. Passerini, *Prospect. Li-ion Battery. Energy. Energy Electrochem. Syst.*, 2018, **4**, 319.

2 J. Xiao, *Science*, 2019, **366**, 426.

3 M. Doyle, T. F. Fuller and J. Newman, *Electrochim. Acta*, 1994, **39**, 2073.

4 S. Feng, D. Shi, F. Liu, L. Zheng, J. Nie, W. Feng, X. Huang, M. Armand and Z. Zhou, *Electrochim. Acta*, 2013, **93**, 254.

5 Q. Ma, Y. Xia, W. Feng, J. Nie, Y. S. Hu, H. Li, X. Huang, L. Chen, M. Armand and Z. Zhou, *RSC Adv.*, 2016, **6**, 32454.

6 L. Porcarelli, A. S. Shaplov, F. Bella, J. R. Nair, D. Mecerreyes and C. Gerbaldi, *ACS Energy Lett.*, 2016, **1**, 678.

7 M. Martinez-Ibañez, E. Sanchez-Diez, L. Qiao, L. Meabe, A. Santiago, H. Zhu, L. A. O'Dell, J. Carrasco, M. Forsyth, M. Armand and H. Zhang, *Batteries Supercaps*, 2020, **3**, 738.

8 G. Luo, B. Yuan, T. Guan, F. Cheng, W. Zhang and J. Chen, *ACS Appl. Energy Mater.*, 2019, **2**, 3028.

9 R. Bouchet, S. Maria, R. Meziane, A. Aboulaich, L. Lienafa, J. Bonnet, T. N. T. Phan, D. Bertin, D. Gigmes, D. Devaux, R. Denoyel and M. Armand, *Nat. Mater.*, 2013, **12**, 1.

10 C. A. Angell, C. Liu and E. Sanchez, *Nature*, 1993, **362**, 137.

11 L. C. Loaiza and P. Johansson, *Macromol. Chem. Phys.*, 2022, **2100419**, 1.

12 N. A. Stolwijk, C. Heddier, M. Reschke, M. Wiencierz, J. Bokeloh and G. Wilde, *Macromolecules*, 2013, **46**, 8580.

13 A. Ferry, P. Jacobsson and J. R. Stevens, *J. Phys. Chem.*, 1996, **100**, 12574.

14 R. Xue and C. A. Angell, *Solid State Ionics*, 1987, **25**, 223.

15 C. Vachon, C. Labrèche, A. Vallée, S. Besner, M. Dumont and J. Prud'homme, *Macromolecules*, 1995, **28**, 5585.

16 G. G. Silva, P. P. De Souza, A. J. S. Mizher and M. A. Pimenta, *Mater. Sci. Forum*, 2005, **480–481**, 273.

17 M. Herstedt, M. Smirnov, P. Johansson, M. Chami, J. Grondin, L. Servant and J. C. Lassègues, *J. Raman Spectrosc.*, 2005, **36**, 762.

18 D. Brouillette, D. E. Irish, N. J. Taylor, G. Perron, M. Odziemkowski and J. E. Desnoyers, *Phys. Chem. Chem. Phys.*, 2002, **4**, 6063.